

Numerical Analysis of Supersonic Flow and Shockwave Behavior Over a Convex Wedge

Nobin Dhar^{}, Mohammad Ilias Inam, Azizul Hakim Aakash*

Department of Mechanical Engineering, Khulna University of Engineering & Technology, Khulna-9203, Bangladesh

ABSTRACT

The present study describes the flow behavior around the leading edge of a convex wedge having a specific dimension under varying upstream Mach numbers ranging from 1.4 to 2. The interaction between the free stream flow and the wedge significantly affects flow parameters such as static pressure, density, static temperature, downstream Mach number, and shock standoff distance (SSD), which are crucial for efficient aerodynamic design. Previously, various researchers have considered the convex wedge flow configuration specifically for inviscid flow but limited attention has been given to the detailed behavior of flow parameters at the leading edge of a convex wedge under varying upstream Mach numbers. The results indicate that, static pressure increased almost 80% at upstream Mach number 2 at the leading edge of the convex wedge. Density, static temperature, downstream Mach number all of them increased by 40%, 28%, and 40% respectively. The downstream Mach number, at first increases slowly but change takes place rather rapidly when the upstream Mach number crosses the value of 1.6. Again, the SSD showed an abrupt change (almost 95% decrease of its initial value at upstream Mach number 2). The leading edge was chosen for this study since it's considered to be the critical design point which experiences the highest thermal and aerodynamic loads due to the shockwave. Evaluating flow behavior at this point is crucial in managing shockwave-induced loads.

Keywords: SSD (Shock Standoff Distance), Convex Wedge, Supersonic flow, CFD, Bow shock



Copyright @ All authors

This work is licensed under a [Creative Commons Attribution 4.0 International License](https://creativecommons.org/licenses/by/4.0/).

1. Introduction

The study of supersonic fluid flow over curved edges is of significant interest in aerospace engineering, as the initial supersonic flow generates shockwaves [1] which directly impacts the aerodynamic performance. Understanding the flow parameters around curved wedge can help to moderate designs of high-speed vehicles and increase performance efficiency. Curved wedges are used as shock generating surfaces to reduce flow stagnation pressure loss and it also promotes pre-combustion flow compression [2].

Curved wedge generates bow shocks, which significantly alters the downstream flow properties. The downstream flow properties alternation factors are mainly upstream Mach number and the curvature of the wedge. And not only the flow property but also the shock standoff distance also varies due to upstream Mach number and curvature of the wedge.

The study of shockwave phenomena and their effects on supersonic and hypersonic flows has been a subject of extensive research, with various analytical, experimental, and computational approaches contributing to this topic. Worku et al. developed theoretical relations for estimating the shock stand-off distance (SSD) using Curved Shock Theory (CST) for blunt and bluff bodies in supersonic and hypersonic flows [3]. Similarly, Surujhal and Skews investigated the effects of curvature on shock behavior, finding that smaller curvatures produce stronger shocks closer to the surface. This results in enhanced post-shock flow compression, with numerical simulations aligning well with experimental data for streamline shapes but showing discrepancies further downstream due to increasing curvature effects. They suggested that curved wedges could reduce stagnation

pressure losses and improve flow compression, offering potential benefits for internal compression intake designs [2]. Mishra et al. conducted experimental studies on SSD in front of acute-angled wedges under supersonic conditions, using water flow channels as an analogy for high-speed gas flows which provided valuable experimental validation of SSD behavior [4]. Numerical simulations have been extensively employed to study shockwave dynamics. Zore et al. utilized ANSYS Fluent to showcase pressure signatures, boundary layer effects, and solution-based mesh adaptation techniques for hypersonic 2D shock interactions. Their work highlighted the importance of adaptive meshing for accurately capturing complex shockwave phenomena [5]. Similarly, Khan et al. simulated and analyzed shockwave behavior for various wedge angles using ANSYS Fluent [6]. The surface pressure distribution over a 2D wedge for various Mach numbers was analyzed by Shaikh et al. where they showed that as Mach number increases, the Mach cone angle decreases, affecting the pressure distribution along the wedge surface [7]. The effects of unsteady dynamics of hypersonic flow over double wedges with varying wedge angles and lengths were explored by Kumar and De, as their study revealed that unsteady separation zones significantly impact wall pressure and heat flux, which has implications for the thermal and structural loads on hypersonic vehicles [8]. The interaction between 2D/3D conical shock and axisymmetric boundary layer at supersonic flow was investigated by Weng et al. [9]. Despite extensive research on planar and convex wedges, the effects of varying upstream Mach numbers on static pressure and temperature, density at the leading edge remain underexplored.

*Corresponding Author Email Address: nobindhar277@gmail.com

The purpose of this study is to investigate numerically the flow characteristics over a convex wedge using computational fluid dynamics (CFD) simulations in ANSYS Fluent. The main focuses are on convex curvature and seven upstream Mach numbers (1.4, 1.5, 1.6, 1.7, 1.8, 1.9 and 2), analyzing the change of parameters such as static pressures and temperatures, downstream Mach numbers, density at the leading edge. Moreover, the shock standoff distance (SSD) is also quantified. Future studies can build on this work to explore viscous effects and extend the analysis to varying curvatures.

2. Methodology

In this particular study, a geometry of convex wedge was chosen. The modeling was done assuming a free stream flow passed through the two-dimensional wedge. The geometry of the wedge was created using DesignModeler in ANSYS program. The Computational Fluid Dynamics (CFD) approach was implemented to carry out a number of simulations, and the results were analyzed. This approach works mainly as a pre-processor, solver, and post-processor. Steady, absolute, 2D planar pressure-based solver was used and the model used here is inviscid.

2.1 Geometry:

The modelling of the geometry was done in ANSYS workbench with the specified dimensions were defined as follows: The horizontal distances a and b were set to 1.5 m and 0.5 m, respectively, while the vertical distance c was 1.259 m. The vertical distance d is depending on the angle θ (in degrees). The value of θ was taken 15° . A perpendicular line was drawn from the midpoint of the inclined line, denoted as l , with a length of 2 m. A circle was then drawn using the bottom point as the center, resulting in the formation of the curved wedge. An external surface was created enabling the analysis of the fluid flow behavior as it interacts with and processes around the wedge [10].

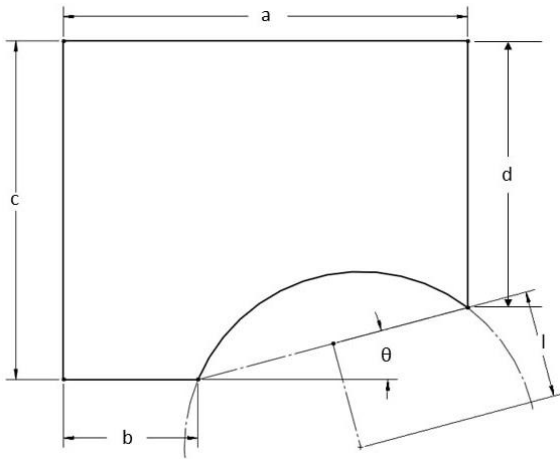


Fig.1 Two-dimensional Geometry of Wedge

2.2 Governing Equations:

The equations of conservation of mass (continuity equation), conservation of momentum, conservation of energy for infinitesimal fluid element and equation of state are given below. The governing equations (Eq. (1) to Eq. (3)) are numerically solved with the help of finite element method.

$$\nabla \cdot (\rho \vec{V}) = 0 \quad (1)$$

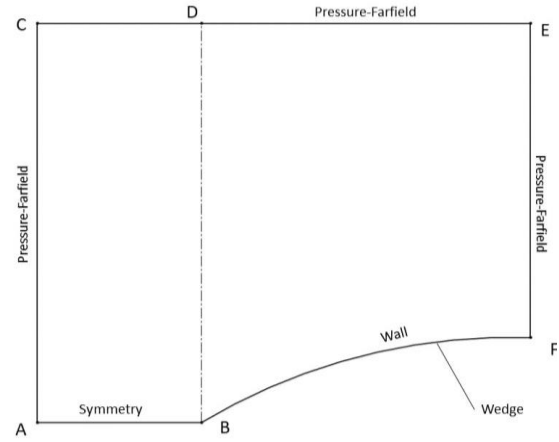
$$\rho(\vec{V} \cdot \nabla) \vec{V} = -\nabla p \quad (2)$$

$$\rho(\vec{V} \cdot \nabla) \left(C_v T + \frac{V^2}{2} \right) = -\nabla \cdot (p \vec{V}) \quad (3)$$

$$P = \rho RT \quad (4)$$

2.3 Computational domain and Boundary Conditions:

The boundary condition for the outer domain ACDEF was selected as pressure-far field where free-stream conditions were set with a free-stream pressure of 1 atm and temperature of 300 K. The velocity was inputted as Mach number (M). Boundary condition for AB and BF were designated as



symmetry and wall types respectively.

Fig.2 Boundary conditions

2.4 Meshing and Analysis:

The meshing of the convex wedge was completed by the software ANSYS Meshing. The meshing was done with quadrilateral elements for the whole surface. To resolve the curved surface of the wedge, the element size was kept small enough [2]. For getting a better solution very fine mesh was created with a structural mesh option. Optimal element size was chosen from the mesh independency test.

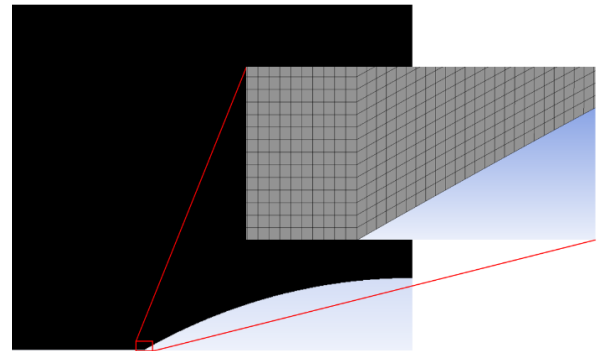


Fig.3 Mesh of the convex wedge

2.5 Mesh Independency:

A series of simulations was carried out for mesh independency test to ensure the accuracy of the numerical results. The goal is to discover a mesh configuration that provides accurate results with marginal computational expense. We created a point at the leading edge of this convex wedge (for $l=2$) and calculated the downstream Mach number ($M_{0.5}$) for this particular point at different element sizes. **Fig.4** shows how the downstream Mach number at leading edge varies with the number of mesh elements for a convex wedge. As can be seen in **Fig.4**, meshes of more than 427120 elements

(element size 0.004 m) are able to generate accurate results with minimal deviation. Consequently, for further simulation, the meshes with element number 427120 was chosen.

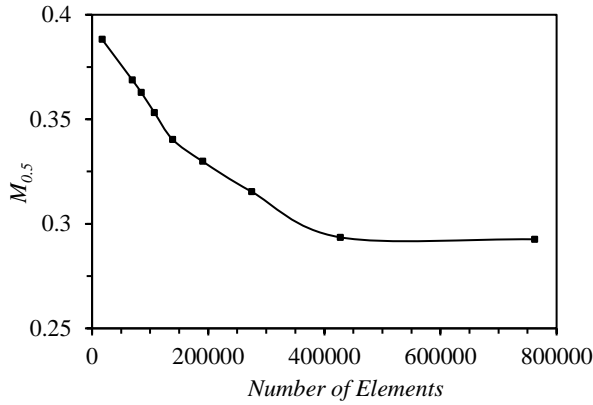


Fig.4 Variation of downstream Mach number at leading edge ($M_{0.5}$) with number of elements

2.6 Validation:

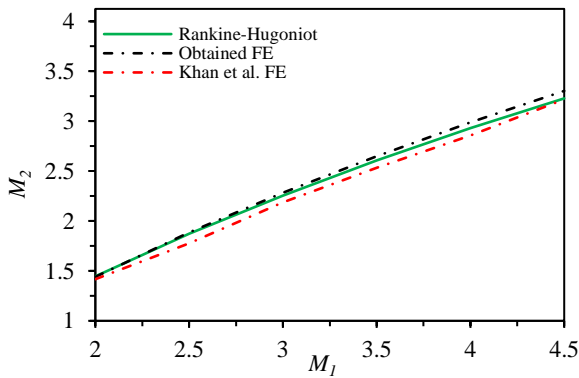


Fig.5 Validation against the values found from Khan et al. for planar wedge

Fig. 5 validates the numerical results for a planar wedge (for $\theta=15^\circ$), comparing downstream Mach numbers against upstream values with theoretical and numerical data from Khan et al. [10]. Theoretical results use Rankine-Hugoniot relations, and the present study shows good agreement with Khan et al.'s findings.

3.0 Results and Discussion:

3.1 Static pressure variation with Mach number:

The graph in **Fig.6** depicts the measured static pressure as a function of upstream Mach number (M_1) at the leading

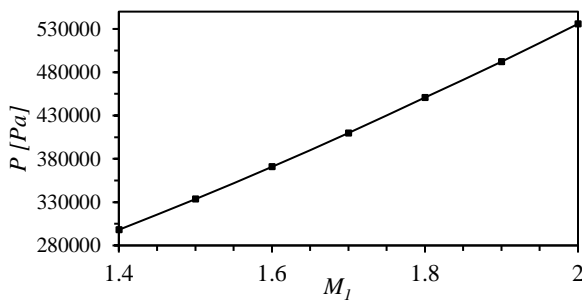


Fig.6 Static pressure variation with upstream Mach number at the leading edge of a convex wedge

edge of the convex wedge within the supersonic range of 1.4 to 2.0. It shows a linear increase in static pressure with upstream Mach number. This trend implies a strong dependency of static pressure with increasing flow velocity which is a common phenomenon in compressible flow over sharp-edged bodies. This rise in pressure is expected to be the result of enhanced compression effects and the variation in shock standoff distance as the Mach number increases.

3.2 Density variation with Mach number:

In order to understand the flow around the wedge the density approach is considered at the leading edge of the wedge. In **Fig.7**, the trend closely resembles the characteristics found in the static pressure curve since it is reflecting the compressibility effects of supersonic flow over a wedge. As the Mach number increases, the flow experiences stronger normal shocks at the leading edge which results simultaneous increase in both density and pressure. However, the increase of the static pressure is larger than the change of density if we compare the changes with upstream conditions.

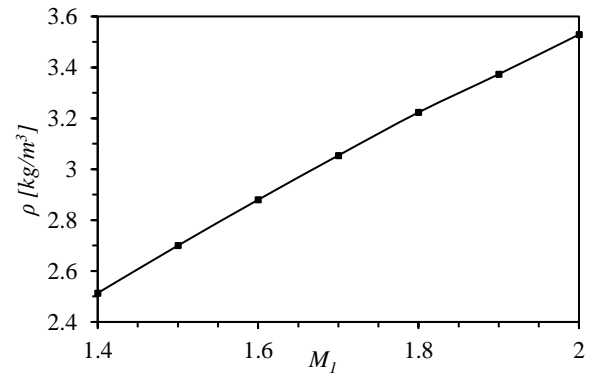


Fig.7 Density variation with upstream Mach number at the leading edge of a convex wedge

3.3 Static temperature variation with Mach number:

From **Fig.8**, it is seen that there's a progressive increase in static temperature with the increase of upstream Mach number same as pressure and density. The static temperature shows a notable increase with the increase of upstream Mach number. The values are changing from 413.144 K at Mach 1.4 to 529 K at Mach 2 with an increase of approximately 28%. This variation in temperature has a big impact on aerodynamic heating, which plays an important role in thermal management of high-speed vehicles.

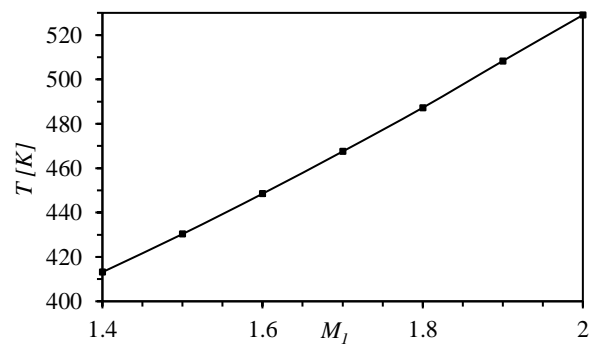


Fig.8 Static temperature variation with upstream Mach number at the leading edge of a convex wedge

3.4 Downstream Mach Number Variation with Upstream Mach Number

In **Fig.9**, it is observed that the downstream Mach number increases non-linearly with the upstream Mach number. For the Mach numbers 1.4-1.6, the increase is negligible. Beyond the point of 1.6, the rise of downstream Mach number is more pronounced. It happens due to the growing compressibility effects. One key observation is that, the downstream Mach number at leading edge is always subsonic for the upstream Mach number ranges considered. This is because the point which is directly in front of the leading edge in the shock wave corresponds to a normal shock [1]. As a result, at the leading edge all the downstream Mach number values are subsonic.

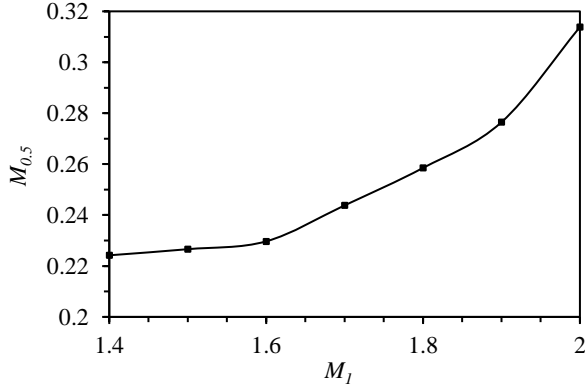


Fig.9 Downstream Mach number ($M_{0.5}$) variation with upstream Mach number at the leading edge of a convex wedge

3.5 Variation of Shock Standoff Distance (SSD) with Mach Number

Shock standoff distance is the perpendicular distance between the leading edge of the convex wedge and the shock wave. From **Fig.10**, we can see that a non-linear decreasing trend taking place as the upstream Mach number increases from 1.4 to 2. At Mach 1.4, the SSD is approximately 0.37739 m, but it reduces sharply, reaching 0.01964 m at Mach 2. The changing of SSD is in an exponential-like decay. As the Mach number increases, the SSD approaches an asymptotic minimum. Because, the strength of the bow shock intensifies as the Mach number increases. As a result, a greater compression and a stronger adverse pressure gradient take place which force the shock wave to move closer to the leading edge.

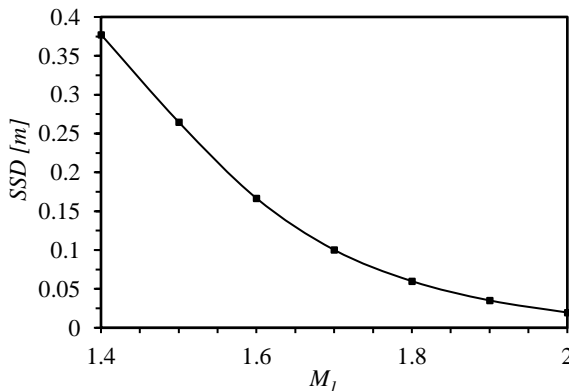


Fig.10 SSD variation with upstream Mach number at the leading edge of a convex wedge

For determining the SSD, Iso-Surfaces were created for the upstream Mach numbers ranging from 1.4 to 2. After that, the Vertex Minimum values were taken from Reports for the Iso-Surfaces which were created earlier.

For an upstream Mach number of 1.7, the bow shock is depicted in **Fig.11**. From the contour, it is evident that the bow shock is extremely thin, typically on the order of a few mean free paths in thickness [1]. This characteristic thinness is a fundamental feature of strong shocks in compressible flows which highlights the sharp transition between the supersonic and subsonic regions.

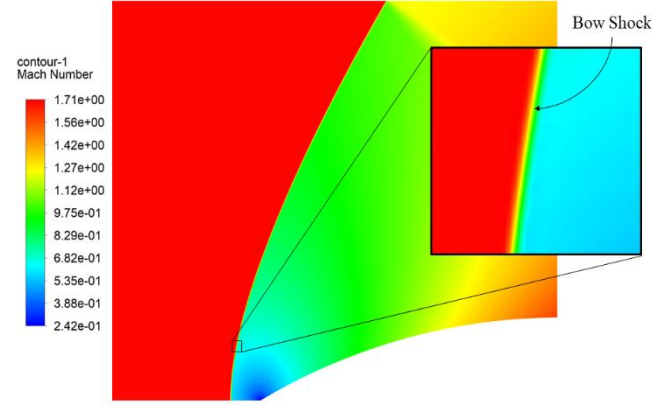


Fig.11 Bow shock for upstream Mach number 1.7

From the contours in **Fig.12(a)** to **Fig.12(c)** i.e. for upstream Mach numbers 1.4-1.6, the bow shock is positioned further from the wedge which results in a larger SSD. The shock gradually moves towards the wedge as the Mach numbers are increased from 1.4 to 1.6. Similarly, for the higher Mach numbers in **Fig.12(d)** to **Fig.12(f)**, the shock is observed to move closer to the convex wedge surface. As a result, the SSD is becoming very small. For Mach number 2 in **Fig.12(f)**, we can see that, the bow shock is almost attached to the surface. This happens due to the increased velocity of the incoming flow which compresses the flow more. So, a steeper pressure gradient at the leading edge of the body takes place which causes the shockwave to move closer to the surface.

At higher Mach numbers, the flow becomes more compressible which enables the flow to adjust more quickly to the presence of the convex wedge. And the increased kinetic energy of the flow allows it to adjust more effectively to the convex wedge. Consequently, the bow shock forms closer to the wedge surface. Also, the thickness of the shock gradually decreases as the Mach number increases which makes it even sharper and more localized. The change in the shock standoff distance can be a significant indicator of the changes in other properties i.e. the drag on an aircraft or the heat flux on a re-entry vehicle [3].

The decrease in SSD has critical implications for the design of aerodynamic vehicles since it enhances the thermal and pressure loads on the body. Understanding this relationship between them is vital for designing re-entry vehicles, heat shields and high-speed aircraft where shockwave-induced heating and stresses are significant.

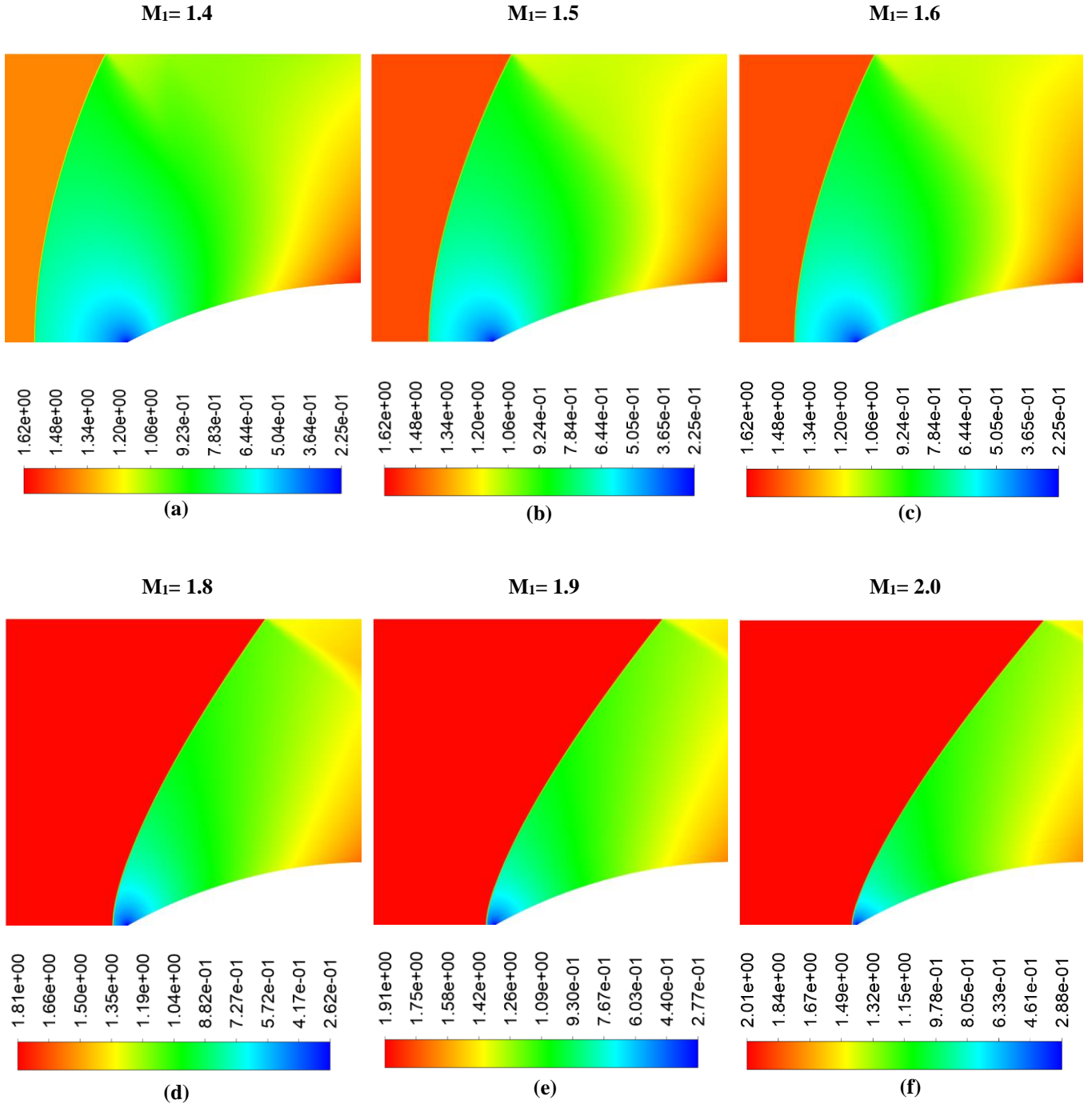


Fig.12 Contours of Mach number distribution around a wedge for different upstream Mach numbers ($M_1 = 1.4$ to $M_1 = 2.0$). Figs. (a)-(f) highlight the variation in the bow shock position and the extent of subsonic regions downstream of the shock as the upstream Mach number increases.

4. Conclusion

This paper explains the variation of key flow parameters at the leading edge of a convex wedge for upstream Mach numbers ranging from 1.4 to 2. Static pressure has been increased from 2.98×10^5 Pa to 5.35×10^5 Pa for the upstream Mach numbers 1.4 to 2. From the values, the increase in static pressure is approximately 80% at upstream Mach number 2. Similarly, density increases from 2.513 kg/m^3 to 3.528 kg/m^3 . For this case, the increase is about 40%. So, static pressure increases more intensely than density. The static temperature follows a similar trend, rising from 413.144 K to 529 K, reflecting an increase of 28%. $M_{0.5}$

increases from 0.2242 to 0.31384 and the increase is about 40%. In contrast, the SSD decreases sharply from 0.378 m to 0.0196 m, indicating a reduction of approximately 95%. This sharp decline in SSD takes place due to the greater compressibility of the flow and the higher velocities encountered at increased upstream Mach numbers.

The results may play a significant role in designing supersonic and hypersonic vehicles, where managing aerodynamic loads, thermal stresses, and shock positions are crucial for better performance and material integrity.

References

- [1] Oosthuizen P.H., Carscallen W. E. Compressible Fluid Flow. THE MCGRAW-HILL COMPANIES, INC.; 1997.
- [2] Surujhlal D, Skews BW. Two-dimensional supersonic flow over concave surfaces. Shock Waves 2018;28:1199–205.
- [3] Worku Z, Timofeev E, Mölder S. Estimation of Shock Stand-off Distance Using the Curved Shock Theory and Its Validation via Numerical Modelling. 2018.
- [4] Mishra A, Khan A, Musfirah Mazlan N. Determination of shock standoff distance for wedge at supersonic flow. International Journal of Engineering, Transactions A: Basics 2019;32:1049–56.
- [5] Zore K, Ozcer I, Munholand L, Stokes J. ANSYS CFD Simulations of Supersonic and Hypersonic Flows. n.d.
- [6] Khan SA, Aabid A, Mokashi I, Al-Robaian AA, Alsagri AS. CFD Letters Optimization of Two-dimensional Wedge Flow Field at Supersonic Mach Number. CFD Letters 2019;11:80–97.
- [7] Shaikh JS, Kumar K, Pathan KA, Khan SA. Computational Analysis of Surface Pressure Distribution over a 2DWedge in the Supersonic and Hypersonic Flow Regimes. Fluid Dynamics and Materials Processing 2023;19:1637–53.
- [8] Kumar G, De A. Role of corner flow separation in unsteady dynamics of hypersonic flow over a double wedge geometry. Physics of Fluids 2021;33.
- [9] Weng Y, Li Q, Tan G, Su W, You Y. Numerical investigations on interactions between 2D/3D conical shock wave and axisymmetric boundary layer at Ma=2.2. Aerosp Sci Technol 2024;144.
- [10] Khan SA, Aabid A. CFD Simulation with Analytical and Theoretical Validation of Different Flow Parameters for the Wedge at Supersonic Mach Number. vol. 19. 2019.

NOMENCLATURE

- p : Static pressure, Pa
- $M_{0.5}$: Downstream Mach Number at leading edge
- ρ : Density, kg/m³
- T : Static temperature, K
- SSD : Shock standoff distance, m
- M_1 : Upstream Mach number
- M_2 : Downstream Mach number